JACS
JOURNAL OF THE AMERICAN CHEMICAL SOCIETY

Article

pubs.acs.org/JACS

Correlations between Mass Activity and Physicochemical Properties of Fe/N/C Catalysts for the ORR in PEM Fuel Cell via ^{57}Fe Mössbauer Spectroscopy and Other Techniques

Ulrike I. Kramm,*[,†,§] Michel Lefèvre,[‡] Nicholas Larouche,[§] Dieter Schmeisser,[†] and Jean-Pol Dodelet*[,§]

[†]Chair of Applied Physics and Sensors, Brandenburgische Technische Universität Cottbus Senftenberg, Konrad-Wachsmann-Allee 17, 03046 Cottbus, Germany

[§]Institut National de la Recherche Scientifique, Énergie, Matériaux et Télécommunications, 1650 Lionel-Boulet Blvd., Varennes, Québec, J3X 1S2, Canada

[‡]Canetique Electrocatalysis Inc., 1650 Lionel-Boulet Blvd., Varennes, Québec, J3X 1S2, Canada

Supporting Information

ABSTRACT: The aim of this work is to clarify the origin of the enhanced PEM-FC performance of catalysts prepared by the procedures described in *Science* **2009**, *324*, 71 and *Nat. Commun.* **2011**, *2*, 416. Catalysts were characterized after a first heat treatment in argon at 1050 °C (Ar) and a second heat treatment in ammonia at 950 °C (Ar + NH_3). For the NC catalysts a variation of the nitrogen precursor was also implemented. ^{57}Fe Mössbauer spectroscopy, X-ray photoelectron spectroscopy, neutron activation analysis, and N_2 sorption measurements were used to characterize all catalysts. The results were correlated to the mass activity of these catalysts measured at 0.8 V in H_2/O_2 PEM-FC. It was found that all catalysts contain the same FeN_4-like species already found in INRS Standard (*Phys. Chem. Chem. Phys.* **2012**, *14*, 11673). Among all FeN_4-like species, only D1 sites, assigned to FeN_4/C, and D3, assigned to N-FeN_{2+2} /C sites, were active for the oxygen reduction reaction (ORR). The difference between INRS Standard and the new catalysts is simply that there are many more D1 and D3 sites available in the new catalysts. All (Ar + NH_3)-type catalysts have a much larger porosity than Ar-type catalysts, while the maximum number of their active sites is only slightly larger after a second heat treatment in NH_3. The large difference in activity between the Ar-type catalysts and the Ar + NH_3 ones stems from the availability of the sites to perform ORR, as many sites of the Ar-type catalysts are secluded in the material, while they are available at the surface of the Ar + NH_3-type catalysts.

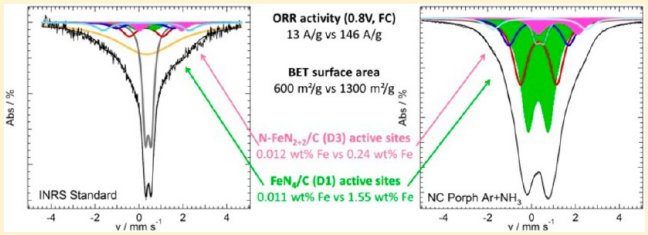

INTRODUCTION

An H_2/O_2 proton exchange membrane (PEM) fuel cell is a generator of electrical power based on the electrochemical oxidation of hydrogen at the anode and the electrochemical reduction of oxygen at the cathode. In these systems, electrocatalysts are necessary to accelerate both half-cell reactions. Today, only platinum and platinum−alloy electrocatalysts are used in all PEM fuel cell prototypes. However, in the context of a strong economy, platinum will always be expensive, hence hindering the large scale commercialization of these clean and efficient electrical energy sources. Today, the platinum catalysts account for 33% of the overall stack costs.[1] Due to kinetic limitations for the oxygen reduction reaction (ORR), the required platinum content at the cathode is about 1 order of magnitude larger than at the anode. Therefore, in terms of cost reduction, the replacement of platinum and platinum−alloy catalysts is especially welcome at the cathode. For the replacement of platinum, a non-noble metal catalyst has to fulfill different requirements: (i) to display an outstanding catalytic activity for the oxygen reduction, (ii) to have sufficient power density in a requested voltage range useful for the targeted application, and (iii) to show long-term stability that is comparable to platinum-based catalysts.

It has been known for several years now that Me/N/C catalysts, prepared by a heat treatment of a source of a nonprecious metal, nitrogen, and carbon can be used as catalysts for ORR in PEM fuel cells.[2−9] Especially during the last 5 years, tremendous progress has been achieved regarding the improvement of the activity, performance and stability of these Me/N/C catalysts, where Me usually is either Fe and/or Co.[10−12] The best stability was demonstrated in 2011 by Fe/Co-PANI-C catalysts that exhibited good long-term performance for 4 weeks of potentiostatic measurement at 0.4 V.[12] A first breakthrough in activity was reported for a Fe/N/C catalyst in 2009.[10] In that work, a highly microporous carbon black was filled by ballmilling the carbon support with a pore filler made of a mixture of phenanthroline and iron acetate, followed by two heat treatments, first in Ar, then in NH_3. This type of Fe/N/C catalyst will be labeled SCI Phen Ar + NH_3 in

Received: October 1, 2013
Published: December 17, 2013

   dx.doi.org/10.1021/ja410076f | *J. Am. Chem. Soc.* 2014, 136, 978−985

this work. A second breakthrough in activity for a Fe/N/C catalyst was published in 2011.[11] In this case the carbon black was substituted by a nitrogen-containing metal organic framework (MOF) that was ballmilled with a mixture of 1,10 phenanthroline and iron acetate. The well-defined initial porous structure of the MOF, after a first pyrolysis in Ar and a second pyrolysis in NH_3, enables also much better mass transport properties and therefore much better performance that approached that of Pt/C in PEM fuel cells. In this work, this second type of Fe/N/C catalyst will be labeled NC Phen Ar (for a catalyst obtained after a pyrolysis in Ar) or NC Phen Ar + NH_3 (for a catalyst obtained after a first pyrolysis in Ar followed by a second pyrolysis in NH_3).

These breakthroughs in Me/N/C catalysts were basically due to the thorough understanding of the structural composition of a long studied Fe/N/C catalyst, labeled INRS Standard, made by heat treating in NH_3 a specific nonporous pristine carbon black impregnated with iron acetate. The study of INRS Standard enabled us to work out the factors which are of importance for the catalyst preparation. These factors are: (i) the concentration and chemical state of nitrogen atoms;[13,14] (ii) the presence of the required porous surface area to obtain a performing catalyst;[15,16] and (iii) the number and electronic state of specific FeN_4 centers, especially those able to perform ORR.[17] The latter study relied heavily on previous studies on other Fe/N/C catalysts.[18−22]

It is well-known that catalysts always achieve much higher current densities after a second heat treatment in NH_3 than after just a single heat treatment in Ar.[10,11,18,22,23] The aim of this work is to clarify how a second heat treatment in NH_3 affects the structural composition and ORR activity of the SCI and different NC catalysts and to compare these results with those already obtained with INRS Standard.

RESULTS AND DISCUSSION

Evaluation of the Activity of All the Catalysts in PEM Fuel Cells. H_2/O_2 fuel cell polarization curves were recorded for all SCI and NC catalysts prepared for this work. These include SCI Phen Ar and SCI Phen Ar + NH_3, NC Phen Ar and NC Phen Ar + NH_3, NC PANI Ar and NC PANI Ar + NH_3 as well as NC Porph Ar and NC Porph Ar + NH_3. For all Ar-pyrolyzed catalysts, nitrogen is provided either by ZIF-8 and/or phenanthroline, PANI, or iron porphyrin. The catalyst activity that will be used in this work is measured at 0.8 V in A g^{-1} of catalyst and is defined as the actual mass activity on the beginning of life polarization curve of each catalyst presented in Figure 1.

Activity values at 0.8 V and the nominal and actual iron loadings determined by neutron activiation analysis (NAA) of all these catalysts are given in Table 1.

It is obvious from Figure 1 that the activity of all the catalysts obtained after a first pyrolysis in Ar (dashed curves) is much lower than that obtained for the same catalysts after a second pyrolysis under NH_3 (solid curves). This is in agreement with the literature on Fe/N/C catalysts.[10,11,18,22−24] The Tafel slopes of all NH_3 treated catalysts are around 65 mV/decade, while they are higher for all Ar-pyrolyzed catalysts (from 95 mV/decade for SCI Phen Ar to 128 mV/decade for NC Phen Ar).

For the sake of comparison we have added Table S1 in the Supporting Information that summarizes mass activity and all structural parameters of the INRS Standard catalyst.

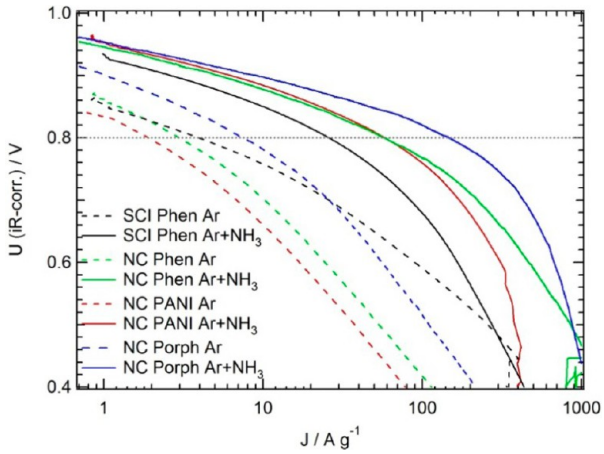

Figure 1. Beginning of life H_2/O_2 fuel cell polarization curves for all the catalysts studied in this work. Mass activities in A g^{-1} (of catalyst) are read at the crossing of each polarization curve with the horizontal dotted line drawn at 0.8 V (iR corrected).

Table 1. Iron Loads (nominal and actual, both in wt %) and Mass Activities (in A g^{-1}) Measured at 0.8 V in H_2/O_2 Fuel Cell for All Fe/N/C Catalysts Studied in This Work

	SCI Phen		NC Phen		NC PANI		NC Porph	
Pyrolysis Gas	1st Ar	2nd NH_3	1st Ar	2nd NH_3	1st Ar	2nd NH_3	1st Ar	2nd NH_3
Nominal Fe load	1.0		1.0		1.0		0.7	
Actual Fe load	1.05	1.37	2.19	4.64	2.71	4.83	1.87	3.55
Mass activity	4.0	25	3.0	60	1.8	60	7.4	146

Structural Characterization of the Catalysts. *Specific Surface Area of the Catalysts.* In polymer electrolyte membrane fuel cells, oxygen reduction takes place at the interface between the catalytic centers and the polymer electrolyte in presence of O_2. Therefore, the catalyst surface area plays a crucial role. N_2 sorption measurements were performed in order to evaluate changes in the total specific surface area (BET) of the catalysts with a change in their preparation procedures. The results are summarized in Table 2.

Table 2. BET Surface Area Determined by N_2 Sorption Measurements, in m^2 g^{-1}, Surface Elemental Composition ([C], [O], [N]), Pyridinic Nitrogen [N_{Pyrid}] and Nominal Nitrogen [N_{Prec}] Contents, measured by XPS, in at %, Given for All Catalysts Studied in This Work

	SCI Phen		NC Phen		NC PANI		NC Porph	
Pyrolysis Gas	1st Ar	2nd NH_3	1st Ar	2nd NH_3	1st Ar	2nd NH_3	1st Ar	2nd NH_3
BET	330	590	330	756	87	619	409	1319
[C]	98.3	97.3	93.0	94.1	92.5	93.5	91.2	91.1
[O]	0.7	0.9	1.9	2.2	2.6	2.1	2.4	2.3
[N]	1.0	1.8	5.1	3.7	4.9	4.4	6.0	6.1
[$N_{Pyrid.}$]	0.4	0.8	2.1	1.8	1.9	2.1	2.7	3.4
[$N_{Prec.}$]	5.2		14.1		12.4		14.8	

dx.doi.org/10.1021/ja410076f | J. Am. Chem. Soc. 2014, 136, 978−985

The important points to notice from this table are that (i) catalysts made under NH_3 are all characterized by a high total specific area (from 590 to 1319 $m^2\ g^{-1}$) similar to that of INRS Standard with ~600 $m^2\ g^{-1}$ (see Table S1) and (ii) the surface areas of all catalysts made under Ar only are either smaller (SCI Phen Ar, NC Phen Ar and NC Porph Ar) or even much smaller (NC PANI Ar) than the surface areas of the catalysts pyrolyzed under NH_3. The mass activity of NC PANI Ar is also the lowest one in Table 1 with 1.8 A g^{-1}.

Surface Composition of the Catalysts Determined by X-ray Photoelectron Spectroscopy (XPS). Besides porosity, the activity of Fe/N/C type catalysts is also very sensitive to the presence of nitrogen atoms at the surface of the catalysts.[14,25] This is because some of these nitrogen atoms are part of the catalytic sites, either as coordinating the iron ion in the FeN_4-like sites or in an eventual combination with the FeN_4-like moiety in the $N-FeN_{2+2}\cdots NH^+$ composite site. The latter site is the most active one in the INRS Standard catalysts.[13,17] The C, O, and N contents, measured by XPS at the surface of the catalysts, are summarized in Table 2. The Fe 2p signal found for some catalysts was not considered due to the low sensitivity for Me 2p.[26]

The important points to notice from the different N surface contents in this table are that: (i) The nitrogen content of the precursors (N_{prec}) of SCI and NC catalysts is much larger than the total nitrogen content measured in the corresponding catalysts after the first pyrolysis in Ar. The highest total nitrogen content in the catalysts is 6.1 at% for NC Porph Ar + NH_3. In that case, about 60% of the nitrogen atoms that were present in the catalyst's precursor were lost upon the first pyrolysis in Ar. (ii) The nitrogen content of SCI Phen Ar + NH_3 is higher than that of SCI Phen Ar. This is the expected behavior for a material heat treated in NH_3, since ammonia is a nitrogen precursor. NH_3 is known to react preferentially with disorganized carbon in carbon black, which is mainly gasified as HCN and H_2 during reaction at temperatures higher than 650 °C.[27,28] On the one hand, for a catalyst like INRS Standard, which is made by pyrolyzing in NH_3 a nonporous furnace carbon black impregnated with iron acetate, this gasification reaction results in a drastic increase of the nitrogen content measured at the surface of the catalyst (from practically no nitrogen for the pristine carbon black impregnated with iron acetate, up to ~2 at% N for INRS Standard; see Table S1). Furthermore, the increase in N content occurs together with an important rise in the porosity of this INRS Standard catalyst (from a BET of about 80 (for the pristine carbon black) to a BET of 600 $m^2\ g^{-1}$; see Table S1). On the other hand, SCI Phen Ar + NH_3 is made with a furnace black (Black Pearls 2000) which is already highly porous.[10] Its pores are first filled with a mixture of iron acetate and phenanthroline before being pyrolyzed in Ar and then in NH_3. Here again, disordered carbonaceous material, which originates either from the highly porous carbon support or from the pyrolyzed phenanthroline, is gasified by NH_3, resulting in an increase of the porosity of the catalyst (from 330 to 590 $m^2\ g^{-1}$), but it is difficult to determine the exact origin of the nitrogen content of the catalyst, as phenanthroline and NH_3 are both nitrogen precursors. Curiously, the final nitrogen content of SCI Ar + NH_3, with its two nitrogen precursors, is lower than that of INRS Standard which has only NH_3 as nitrogen precursor. (iii) The nitrogen content of NC Phen Ar + NH_3 and NC PANI + NH_3 is lower than that of the corresponding catalysts pyrolyzed under Ar only, while for NC Porph Ar + NH_3 the nitrogen content is practically the same as for NC Porph Ar. This is again rather unexpected. However, in this case there is no starting carbon black support, as the NC Ar catalysts are obtained by pyrolyzing under Ar a mixture of ZIF-8, iron acetate, and phenantroline (or alternatively PANI or ClFeTMPP). According to Table 2, the NC catalysts pyrolyzed only in Ar are characterized by a relatively low porosity and by a high nitrogen content that may originate from either the pyrolysis of ZIF-8 or phenantroline (or PANI or ClFeTMPP). When these materials are further pyrolyzed in NH_3, their porosity increases, sometimes drastically like for PANI, but their nitrogen content either decreases (for NC Phen Ar + NH_3 or NC PANI Ar + NH_3) or remains constant (for NC Porph Ar + NH_3).

Both effects observed in (ii) and (iii), that is, an unexpected lower N content in SCI Phen Ar + NH_3 compared with the N content in INRS Standard and no further increase of the N content in NC Ar + NH_3 compared with the N content in the respective NC Ar catalysts, may possibly be explained by the presence of iron carbides detected by Mössbauer spectroscopy in the catalysts (as will be detailed in the next section). Recently it was indeed shown that the occurrence of iron carbide, which is an intermediate in the graphitization of carbon in the presence of iron, leads to the release of HCN fragments (from FeN_4-like centers).[29] A sulfur addition previous to the heat treatment or the interruption of the heat treatment at 500 °C, to acid leach excess iron before resuming the pyrolysis, limits the formation of iron carbide and destruction of FeN_4-type sites.[29−31]

A larger content of iron carbide in the catalyst obtained after the second pyrolysis in NH_3 would therefore lead to a lower total N content than would be expected in the absence of iron carbide. As will be seen later on, there is an increase of more than 0.3 wt % Fe in the form of iron carbide for the SCI Ar + NH_3, NC Phen Ar + NH_3, and NC PANI Ar + NH_3 catalysts compared with the Ar version of the same catalysts, while no iron carbide was detected in INRS Standard[17] and in NC Porph Ar + NH_3. It is in the latter catalyst that the highest nitrogen content (6.1 at % N) has been found. Another important conclusion from Table 2 is that for all the NC type catalysts, the second pyrolysis in NH_3 has only one essential consequence, that of increasing the porosity of the catalysts obtained after the first pyrolysis in Ar but not that of increasing the total N content above the value measured after the first pyrolysis in Ar, as one might have expected based on the fact that NH_3 was previously recognized as a nitrogen precursor to obtain Fe/N/C catalysts. A similar conclusion was also previously reached for porphyrin-based catalysts for which a second heat treatment in NH_3 at 800 °C did not necessary increase the nitrogen content of these catalysts.[22]

^{57}Fe Mössbauer Spectroscopic Analysis of the Catalysts. Mössbauer spectroscopy is a powerful tool for the identification of iron species. It is especially effective for iron species of similar coordination environment but with different electronic states, as for instance in electronically different FeN_4 centers in porphyrins or phthalocyanines. The Mössbauer spectra of SCI Phen and NC catalysts obtained after either a first pyrolysis in Ar or a second pyrolysis in NH_3 are compared in Figure 2.

In order to obtain a reasonable fit to the experimental spectra, three sextets, up to six doublets and one singlet were used in the deconvolutions. The assignment of each sextet, doublet, or singlet to a specific Fe-species and their related parameters is summarized in Table 3. Some of these doublets

dx.doi.org/10.1021/ja410076f | J. Am. Chem. Soc. 2014, 136, 978−985

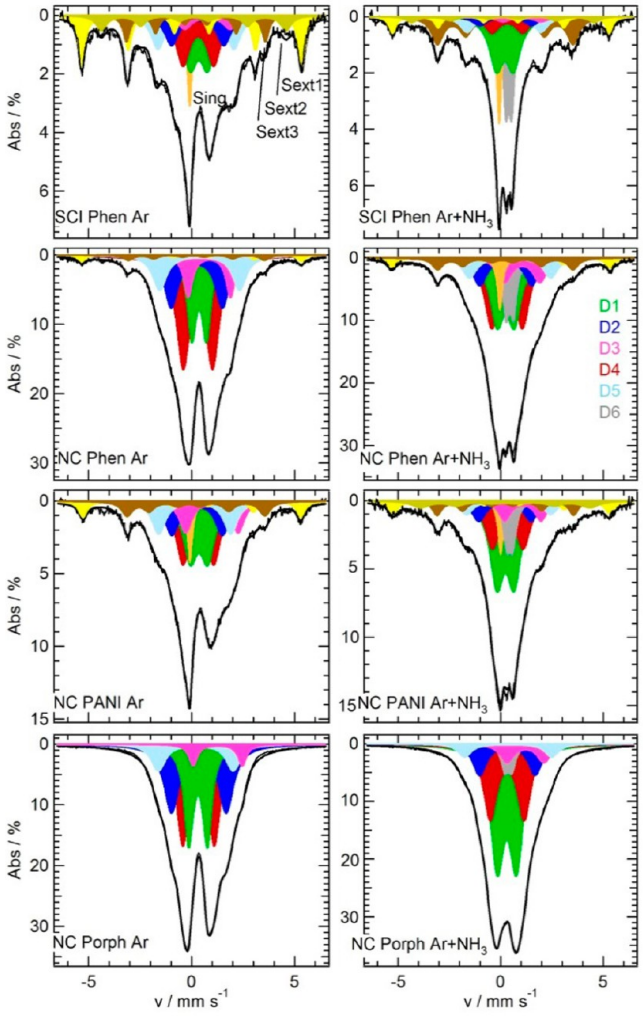

Figure 2. ^{57}Fe Mössbauer spectra of the catalysts obtained after the first heat treatment in Ar (left column) and after the second heat treatment in NH_3 (right column). The color code is the same as that used in Table 3.

(D1, D2, D3, and D6) were already detected in INRS Standard. For the sake of comparison the color code of the different iron sites is the same as that already used in ref 17.

The three sextets and the singlet in Figure 2 are all attributed to inorganic Fe-species like α-iron and/or iron carbide. The latter can be seen in the TEM images presented in the TEM of the Catalysts section. The magnetic fields of these inorganic Fe-species depend on their local coordination environment, which is not the same for all iron sites in iron carbide. In the cases of the singlet, the particle sizes are reduced to a size at which the magnetic interaction vanished. As it was not possible to remove these inorganic species by acid washing we expect that these inorganic particles are completely surrounded by carbon layers and are therefore larger than 1.5 nm in size to be able to stabilize carbon encapsulation.[32] This will be confirmed by the TEM micrographs presented in the TEM of the Catalysts section. By systematic studies it was possible to exclude any catalytic activity toward ORR of such encapsulated iron species in an acid medium.[33,34]

As far as the six doublets are concerned, D6 is also an inorganic species assigned to Fe_xN, with $x \leq 2.1$.[35] This iron nitride species only appears when NH_3 is used in the synthesis procedure of the catalysts. The other five doublets have an

Table 3. Average Mössbauer Parameters Determined for the Different Iron Sites in SCI Phen, NC Phen, NC PANI, and NC Porph Catalysts and the Assignment to Iron Species[a]

	δ_{Iso}	ΔE_Q	H_0	fwhm	Assignment
Site	/ mm s^{-1}		/ T	/ mm s^{-1}	
Sing	-0.06 (0.04)	-	-	0.30 (fixed)	superparamagnetic iron [40]
D1	0.30 (0.06)	0.86 (0.07)	-	0.73 (0.13)	$Fe^{II}N_4/C$, low spin [20,37]
D2	0.27 (0.04)	2.56 (0.09)	-	0.79 (0.04)	$Fe^{II}N_4$, like FePc [41,42]
D3	0.98 (0.15)	1.94 (0.19)	-	0.63 (0.11)	N-$Fe^{II}N_{2+2}$/C, high spin [17]
D4	0.32 (0.02)	1.52 (0.07)	-	0.80 (0.01)	N-($Fe^{III}N_4$)-CN, low spin [43]
D5	0.34 (0.10)	3.92 (0.21)	-	0.79 (0.04)	$Fe^{III}N_4$, intermediate spin (with one or two axial ligands (e.g. p-toluenesulfonate)) [42,44]
D6	0.42 (0.04)	0.33 (0.04)	-	0.40 (0.05)	Fe_xN with $x < 2.1$ [21,22,35]
Sext 1	-0.01 (0.02)	0.02 (0.01)	32.9 (0.2)	0.47 (0.08)	alpha-iron [40]
Sext 2	0.15 (0.06)	-0.01 (0.01)	27.1 (1.2)	0.73 (0.23)	alpha-iron or iron carbide Fe_3C [40]
Sext 3	0.15 (0.07)	0.07 (0.07)	20.6 (0.2)	0.56 (0.10)	iron carbide [40]

[a]Errors are given between parentheses. See Supporting Information for the meaning of δ_{Iso}, ΔE_Q, H_0, and fwhm.

organic origin. They have been assigned to FeN_4-like centers of different electronic states due to changes in their coordination environment and/or different oxidation states. D1 is the well-known signature of the site active for ORR in catalysts obtained by heat-treating supported or unsupported porphyrins.[20−22,36−38] D1 (FeN_4/C) is also known from other Fe/N/C preparation approaches.[17,39] In this site, the iron ion is in the Fe^{II} low-spin state ($S = 0$),[20] and its turnover frequency was found to depend on the electron density on the iron centers.[21]

Doublet D3 (N-FeN_{2+2}/C), in its high activity state (N-FeN_{2+2}···NH^+), was found to be the most active site for the ORR in INRS Standard catalysts.[17] In that state, its turnover frequency of 11.4 e^- per site per second at 0.8 V vs RHE is 2 orders of magnitude larger than that of D1.[20−22] This high turnover frequency is attributed to a close interaction between the FeN_4-like site with NH^+ that is located in the vicinity of the Fe center in the composite catalytic site.[13] In such a configuration, the protonated basic nitrogen (or nitrogen atoms) near N-FeN_{2+2} may serve as a relay to quickly provide the protons that are necessary for the nearby N-FeN_{2+2} moiety to perform ORR. In D3, the Fe^{II} ion is in the high spin state ($S = 2$).

Regarding the three other FeN_4 configurations, so far no significant catalytic activity has been attributed to the FeN_4-centers assigned to doublet D2.[17,20−22] This was explained on the basis of the spin state of D2.[17] As far as D4 and D5 are concerned, these FeN_4-like centers have been assigned (Table 3) to Fe^{III} with one or two axial ligands. This precludes ORR since DFT calculation shows that the direct reduction of O_2 starts by its adsorption on a Fe^{II} ion.[2,3,45]

dx.doi.org/10.1021/ja410076f | J. Am. Chem. Soc. 2014, 136, 978−985

Table 4 summarizes the relative absorption areas (Abs-X) and the iron concentrations assigned to each iron species (Fe-

Table 4. Summary of the Relative Absorption Areas (X-A) and of the Iron Concentrations Assigned to Each Iron Species (X-Fe) Found in Figure 2[a]

	SCI Phen		NC Phen		NC PANI		NC Porph	
Pyrolysis gas	1st Ar	2nd NH_3	1st Ar	2nd NH_3	1st Ar	2nd NH_3	1st Ar	2nd NH_3
$Fe_{abs.}$/ wt%	1.05	1.37	2.19	4.64	2.71	4.83	1.87	3.55
Sing-A / %	5.9	9.2	-	3.8	4.4	3.9	-	-
Sing-Fe / wt%	0.06	0.13	-	0.18	0.12	0.19	-	-
D1-A / %	16.6	21.7	18.0	22.9	21.8	29.6	23.2	43.6
D1-Fe / wt%	0.17	0.30	0.39	1.06	0.59	1.43	0.44	1.55
D2-A / %	10.2	4.0	18.2	10.4	13.8	7.8	19.2	11.8
D2-Fe / wt%	0.11	0.06	0.40	0.48	0.37	0.38	0.36	0.42
D3-A / %	4.6	2.2	9.5	8.9	8.4	6.6	9.0	6.8
D3-Fe / wt%)	0.05	0.03	0.21	0.41	0.23	0.32	0.17	0.24
D4-A / %	16.6	7.2	37.5	25.4	22.8	17.6	38.7	27.8
D4-Fe / wt%	0.17	0.10	0.82	1.18	0.62	0.85	0.73	0.99
D5-A / %	11.6	7.0	12.3	7.5	12.8	5.3	9.9	5.0
D5-Fe / wt%	0.12	0.10	0.27	0.35	0.35	0.26	0.19	0.18
D6-A / %	-	16.0	-	10.0	-	7.8	-	5.0
D6-Fe / wt%	-	0.22	-	0.46	-	0.38	-	0.18
Sext1-A / %	17.8	7.6	2.2	4.6	7.5	7.3	-	-
Sext1-Fe / wt%	0.19	0.10	0.05	0.21	0.20	0.35	-	-
Sext2-A / %	7.8	3.9	-	-	-	6.5	-	-
Sext2-Fe / wt%	0.08	0.05	-	-	-	0.31	-	-
Sext3-A / %	9.0	21.3	2.2	6.5	8.6	7.6	-	-
Sext3-Fe / wt%	0.10	0.29	0.05	0.30	0.23	0.37	-	-

[a]The actual iron load of each catalyst (Fe_{abs}) is also given.

species X) found in Figure 2. The actual iron load of each catalyst (Fe_{abs}) is also given in Table 4. Figure 3 groups the results given in Table 4 for the relative absorption areas and Fe contents of inorganic iron species (Singlet + D6 + Sext1 + Sext2 + Sext3) and of FeN_4-like iron species (D1 + D2 + D3 + D4 + D5) for all the iron compounds found in Figure 2. The important points to notice from Tables 4 and Figure 3 are that (i) the nominal loading of all the catalysts was about 1 wt % Fe. However, in Table 4, the total iron load (Fe_{abs}) for all the catalysts is always greater than 1 wt % because some mass (essentially carbon, oxygen and nitrogen, but no iron) is lost

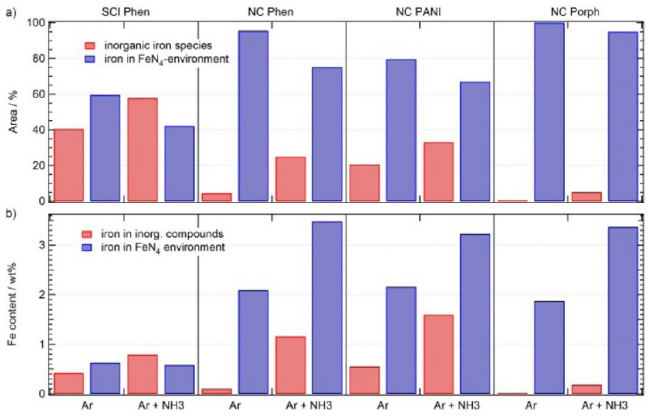

Figure 3. Category plots of the sum of relative absorption areas (a) and iron contents (b) assigned to inorganic iron species (Singlet + D6 + Sext1 + Sext2 + Sext3) and assigned to iron in FeN_4-like environment.

during each pyrolysis step necessary to obtain the catalysts. The mass lost after the first pyrolysis in Ar is 25 wt % for SCI Phen Ar and 65 wt % for all NC Ar catalysts. An additional mass loss of 25% of the mass left after the first pyrolysis is observed for SCI Phen Ar + NH_3, while the additional mass loss is of 50 wt % for all NC Ar + NH_3 catalysts. NH_3 is well-known to gasify carbon at the temperatures used to produce the catalysts.[27,28] (ii) In Figure 3, the relative absorption areas of inorganic iron species increase going from a pyrolysis in Ar to a pyrolysis in Ar + NH_3, for all SCI and NC catalysts. Furthermore, the relative absorption areas of inorganic iron decreases in the order SCI Phen > NC PANI > NC Phen > NC Porph (either Ar or Ar + NH_3). Accordingly, of course, the relative absorption areas related to FeN_4-like iron species display the opposite behavior. Their relative contributions are smaller after the second heat treatment in NH_3. This is an important observation since the catalytic sites are found among the organic FeN_4-like iron species. (iii) In Figure 3, the iron contents (wt %) related to a FeN_4-like environment are quite similar in NC Phen Ar, NC PANI Ar, and NC Porph Ar (about 2.0 wt %). This is also true for the contents in NC Phen Ar + NH_3, NC PANI Ar + NH_3, and NC Porph Ar + NH_3 (about 3.4 wt %). Furthermore, Fe-organic in all NC catalysts is much larger than that in the two SCI catalysts.

TEM of the Catalysts. TEM was performed in order to ascertain the presence of Fe-containing particles in the catalysts. These particles are either nitrides, like Fe_xN with $x < 2.1$ assigned to D6 in Table 4, or α-iron or iron carbides assigned to Sextets 1−3 (Sext1, Sext2, Sext3) in the same table. Alpha iron or iron carbides usually display irregular shapes and are surrounded by layers of carbonaceous or graphitic materials, while iron nitrides are usually spherical and are oxidized at their surface.[17,46] Two large spherical iron nitride particles are visible on the micrograph of NC PANI Ar + NH_3 in Figure 4a, while the much smaller particles in the same micrographs are either α-iron or iron carbide. Small iron carbides or α-iron particles are also visible on the micrograph of SCI Phen Ar + NH_3 (Figure 4b). A typical iron or iron carbide particle surrounded by graphitic material (Figure 4c) is singled out in the micrograph of the same catalyst. More micrographs for SCI Phen Ar and NC Porph Ar are shown in the Supporting Information. They show typical multiwalled carbon nanotubes that can also be found in the catalysts of this work (Figures S2).

dx.doi.org/10.1021/ja410076f | J. Am. Chem. Soc. 2014, 136, 978−985

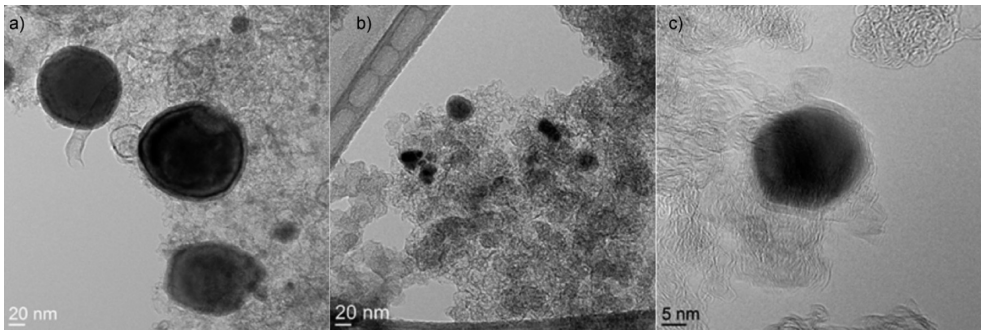

Figure 4. Transmission electron microscopy images of catalysts (a) NC PANI Ar + NH_3, (b) SCI Phen Ar + NH_3, and (c) detail of SCI PhenAr + NH_3.

The observation of Fe-based particles by TEM, and their identification as iron carbide or nitride is basically in agreement with the Mössbauer spectroscopic results. From TEM observations, the following conclusions are drawn: (i) the particle distribution over the catalysts is always inhomogeneous; (ii) no iron nitride particles are detected for the catalysts heat-treated in Ar only and no iron particles of any kind are detected in the NC Porph Ar catalyst (in agreement with the absence of inorganic iron in the Mössbauer spectrum of NC Porph Ar in Figure 3); (iii) the overall particle content is always much higher after the NH_3-treatment step, confirming the much higher content of inorganic iron after this second heat treatment (in agreement with statement (i) of section 2c). This observation seems reasonable, as the additional heat treatment step allows particle diffusion and agglomeration during the second heating step; (iv) the trends in particle growth induced by the second heat treatment in NH_3 for the different preparation approaches are not the same. For example, the SCI Phen Ar catalyst has the largest particles of all Ar-only catalysts but the smallest particles among the Ar + NH_3 catalysts. Hence, this could be an indication that the stabilization of particles during heat treatment on a commercial carbon is easier than the stabilization of similar particles on in situ formed carbon occurring in all NC catalysts.

Correlation between Catalytic Activity in PEM Fuel Cell and Structure of the Catalysts. In the previous section, we said that among all Fe-species present in the catalysts that were analyzed during this work, only species assigned to D1 and D3 are ORR active. The same conclusion was already reached for INRS Standard.[17] If all D1 and D3 active sites were homogeneously distributed in the carbon matrix of the catalyst and were also all able to perform ORR, being fed with oxygen and protons, a linear correlation should therefore exist between mass activity (J/ A g^{-1}) and Fe(D1) or Fe(D3), which are the iron concentrations assigned either to iron in D1 or D3 active sites. Figure 5A,B shows the plots of J vs Fe(D1) or J vs Fe(D3) for the catalysts obtained after two heat treatments (Ar + NH_3) and after a single heat treatment (Ar), respectively. Data for INRS Standard, a catalyst obtained after a single heat treatment in NH_3, were also added to Figure 5A.

It is clear, on the one hand, from Figure 5A, that there is a definite tendency for an increase in mass activity with either an increase of Fe(D1) or Fe(D3). The relative error is, however, still considerable (38% for Fe(D1) and 101% for Fe(D3)). On the other hand, there is no correlation between J and Fe(D1) or Fe(D3) in Figure 5B.

Mössbauer spectroscopy is a bulk characterization technique, and the absolute value of Fe(D1) or Fe(D3) attributed to these

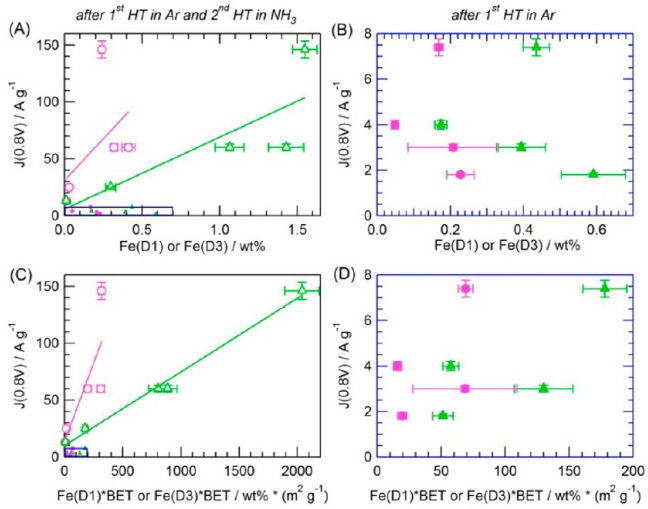

Figure 5. Mass activity at 0.8 V vs (A) Fe(D1) or Fe(D3) and (C) BET × Fe(D1) or BET × Fe(D3) for all catalysts involving a pyrolysis step in NH_3 during their synthesis (open symbols) and (B and D) for all catalysts involving only a pyrolysis step in Ar (filled symbols). Note that the small blue rectangles in (A and C) contain entirely (B and D), respectively. The color code is the same as in Figure 2.

FeN_4-like sites does not necessarily mean that all D1 or D3 sites are able to perform ORR as some of them, not being at the surface of the catalyst, will not be fed either with oxygen or/and protons. If only the sites located close to or at the surface of the catalyst are ORR active, a linear correlation is then expected between J and Fe(D1) × BET or J and Fe(D3) × BET, since a large BET value enhances the probability for D1 or D3 to be at or near the surface of the catalyst where ORR is possible. Figure 5C,D shows the plots of J vs Fe(D1) × BET or J vs Fe(D3) × BET for the catalysts obtained after two heat treatments (Ar + NH_3) and after a single heat treatment (Ar), respectively. Data from INRS Standard were again integrated in Figure 5C.

The much better correlation (5.3%) obtained for D1 in Figure 5C suggests that most of the sites assigned to D1 are located close to or at the surface of the catalysts prepared after two heat treatments (Ar + NH_3). For the same catalysts, the relative error found for Fe(D3) (41.4%) is much larger, meaning that at least some D3 sites are located deeper in the micropores or are secluded in the carbon matrix, where they do not participate in the ORR. The general trend of the experimental data in Figure 5D and their large dispersion for both D1 and D3 sites indicate that, in the catalysts obtained after only one heat treatment in Ar, a large percentage of D1 and D3 sites are secluded in the mass of the catalysts without

dx.doi.org/10.1021/ja410076f | J. Am. Chem. Soc. 2014, 136, 978−985

any possibility to participate in the ORR. This is also the reason why the initial mass activity of these catalysts is so low despite the number of their D1 and D3 sites, which is not so different from the number of D1 and D3 sites found in the catalysts prepared after a first pyrolysis in Ar and a second one in NH_3 (see Table 4). Indeed, by comparing also the two abscissae in Figure 5A,B, one sees that the maximum value of Fe(D1) is only 2.6 times larger in catalysts made in Ar + NH_3 than the maximum value of Fe(D1) for the catalysts made in Ar. For Fe(D3), it is only 1.5 times larger.

In each frame of Figures 5, we have attributed the entire mass activity (J) of the catalysts to either D1 or D3 sites, as we do not know, for each specific figure, the exact fraction of activity (f1 J) attributable to D1 and that (f3 J) attributable to D3. This is not a problem as long as f1 and f3 remain the same for all catalysts used in each one of these figures.

CONCLUSIONS

In this work four different precursor mixtures were used for the preparation of Fe/N/C catalysts. Two preparation routes are similar to the ones described in *Science* and *Nat. Commun.*[10,11] The other two are modifications of the *Nat. Commun.* preparation, where either phenanthroline was exchanged by polyaniline or phenanthroline plus iron acetate were exchanged by chloro-iron tetramethoxyphenylporphyrin (ClFeTMPP). The catalysts were characterized after a first pyrolysis in argon (Ar) and after a second pyrolysis in ammonia (Ar + NH_3).

All catalysts studied in this work display some catalytic activity for the reduction of O_2 in fuel cells. They are however characterized by quite different mass activities at 0.8 V in H_2/O_2 fuel cells. All the catalysts in this work contain similar organic and inorganic Fe-based species and their Mössbauer spectra can be deconvoluted using five doublets of FeN_4-like species. A certain number of Fe-species of inorganic origin (superparamagnetic iron, iron metal, nitride, or carbide) may also be present in some of the catalysts.

Among all the FeN_4-like species ORR activity is only attributed to D1 and D3. D1 has been assigned to FeN_4/C, a well-known site typically found in heat-treated carbon supported or unsupported porphyrins. D3 (N-FeN_{2+2}/C) was so far specific to INRS Standard. In that catalyst, it has been assigned to a very active composite N-FeN_{2+2}···NH^+ site. All Fe-based inorganic species that were identified were found to be ORR inactive.

The percentage of D1 and D3 sites goes from 8.6% for INRS Standard to a maximum of 50.4% for NC Porph Ar + NH_3. For the same catalysts, the absolute iron concentration Fe(D1 + D3) increases from 0.023 wt % to a maximum of 1.79 wt %. Hence, the difference between INRS Standard and the new catalysts pyrolyzed in Ar + NH_3 in this work is that more D1 and D3 sites are available in the new catalysts. The gas used during the pyrolysis step of the new catalysts has a very large influence on the mass activity of the catalysts, but its influence on the number of D1 and D3 sites is only moderate. Indeed, as far as all NC catalysts are concerned, Fe(D1) is on the average 2.6 times larger for all NC Ar + NH_3 heat-treated catalysts than for all NC Ar catalysts. Similarly, it is only 1.5 times larger for Fe(D3). On the contrary, the mass activity resulting from the combined reaction of D1 and D3 types of sites with oxygen is on the average 22 times larger for all NC Ar + NH_3 heat-treated catalysts than for all NC Ar catalysts. This large difference in ORR activity compared with the small difference (factors of 2.6 or 1.5 for Fe(D1) or Fe(D3) in Fe^{II} ions in D1 and D3 active sites, respectively) can be explained in terms of differences in accessibility of O_2 and H^+, or both, to the catalytic sites in Ar and Ar + NH_3 heat-treated catalysts. All catalysts heat-treated in NH_3 during their synthesis have a much larger porosity than those heat-treated in Ar only. Therefore, we deduce that most of the active sites of the new Ar + NH_3 catalysts are located at the surface of the catalysts where they are reachable by O_2 and H^+, while most of the D1 and D3 sites of the catalysts that are only pyrolyzed in Ar are secluded inside the catalytic material and are therefore not available for ORR.

ASSOCIATED CONTENT

Supporting Information

Experimental part and summary of previously obtained structural results for INRS Standard (Table S1) as well as fit results for the Mössbauer spectrum of this catalyst assuming the presence of the same iron sites as in this work (Table S2 and Figure S1). Furthermore, additional TEM images of some catalysts (Figure S2) have been added to highlight the formation of different carbon morphologies depending on the precursor mixtures. This material is available free of charge via the Internet at http://pubs.acs.org.

AUTHOR INFORMATION

Corresponding Authors

kramm@tu-cottbus.de
dodelet@emt.inrs.ca

Notes

The authors declare no competing financial interest.

ACKNOWLEDGMENTS

Dr. D. Alber and G. Bukalis from the Helmholtz-Centre Berlin for Materials and Energy are gratefully acknowledged for the Neutron Activation Analysis (NAA) of the catalysts. This work was supported by funds provided by NSERC, the Canadian funding agency, and by MESRST from the "Gouvernement du Québec".

REFERENCES

(1) de Frank Bruijn, A.; Janssen, G. J. M. In *Encyclopedia of Sustainable Science and Technology*; Meyers, R. A., Ed.; Springer: New York: 2013, p 7694.

(2) Dodelet, J.-P. In *N_4-Macrocyclic Metal Complexes*; Zagal, J. H., Bedioui, F., Dodelet, J.-P., Eds.; Springer: New York, 2006, p 83.

(3) Dodelet, J.-P. In *Lecture Notes in Energy - Electrocatalysis in Fuel Cells*; Shao, M., Ed.; Springer: New York, 2013; Vol. 9, p 271.

(4) Elbaz, L.; Wu, G.; Zelenay, P. In *Lecture Notes in Energy - Electrocatalysis in Fuel Cells*; Shao, M., Ed.; Springer: New York, 2013; Vol. 9, p 213.

(5) Garsuch, A.; Bonakdarpour, A.; Liu, G.; Yang, R.; Dahn, J. R. *Time to move beyond transition metal-N-C catalysts for oxygen reduction*; Wiley: Chichester, U.K., 2009; Chapter 5.

(6) Higgins, D.; Chen, Z. In *Lecture Notes in Energy - Electrocatalysis in Fuel Cells*; Shao, M., Ed.; Springer: New York, 2013; Vol. 9, p 247.

(7) Jaouen, F.; Proietti, E.; Lefèvre, M.; Chenitz, R.; Dodelet, J.-P.; Wu, G.; Chung, H. T.; Johnston, C. M.; Zelenay, P. *Energy and Environmental Science* **2011**, *4*, 114.

(8) Johnston, C. M.; Piela, P.; Zelenay, P. In *Handbook of Fuel Cells – Fundamentals, Technology and Applications*; Vielstich, W., Yokokawa, H., Gasteiger, H. A., Eds.; Wiley: Chichester, U.K., 2009; Vol. 5, Chapter 4, pp 48.

(9) Kramm, U. I.; Bogdanoff, P.; Fiechter, S. In *Encyclopedia of Sustainability Science and Technology*; Meyers, R. A., Ed.; Springer Science+Business Media, LLC: New York, 2013, p 8265.
(10) Lefèvre, M.; Proietti, E.; Jaouen, F.; Dodelet, J.-P. *Science* **2009**, *324*, 71.
(11) Proietti, E.; Jaouen, F.; Lefévre, M.; Larouche, N.; Tian, J.; Herranz, J.; Dodelet, J.-P. *Nat. Commun.* **2011**, *2*, 416.
(12) Wu, G.; More, K. L.; Johnston, C. M.; Zelenay, P. *Science* **2011**, *332*, 443.
(13) Herranz, J.; Jaouen, F.; Lefevre, M.; Kramm, U. I.; Proietti, E.; Dodelet, J.-P.; Bogdanoff, P.; Fiechter, S.; Abs-Wurmbach, I.; Bertrand, P.; Arruda, T.; Mukerjee, S. *J. Phys. Chem. C* **2011**, *115*, 16087.
(14) Lalande, G.; Côté, R.; Guay, D.; Dodelet, J.-P.; Weng, L. T.; Bertrand, P. *Electrochim. Acta* **1997**, *42*, 1379.
(15) Charreteur, F.; Jaouen, F.; Ruggeri, S.; Dodelet, J.-P. *Electrochim. Acta* **2008**, *53*, 2925.
(16) Jaouen, F.; Lefèvre, M.; Dodelet, J.-P.; Cai, M. *J. Phys. Chem. B* **2006**, *110*, 5553.
(17) Kramm, U. I.; Herranz, J.; Larouche, N.; Arruda, T. M.; Lefévre, M.; Jaouen, F.; Bogdanoff, P.; Fiechter, S.; Abs-Wurmbach, I.; Mukerjee, S.; Dodelet, J.-P. *Phys. Chem. Chem. Phys.* **2012**, *14*, 11673.
(18) Koslowski, U. I.; Herrmann, I.; Bogdanoff, P.; Barkschat, C.; Fiechter, S.; Iwata, N.; Takahashi, H.; Nishikoro, H. *ECS Trans.* **2008**, *13*, 125.
(19) Herrmann, I.; Kramm, U. I.; Fiechter, S.; Bogdanoff, P. *Electrochim. Acta* **2009**, *54*, 4275.
(20) Koslowski, U. I.; Abs-Wurmbach, I.; Fiechter, S.; Bogdanoff, P. *J. Phys. Chem. C* **2008**, *112*, 15356.
(21) Kramm, U. I.; Abs-Wurmbach, I.; Herrmann-Geppert, I.; Radnik, J.; Fiechter, S.; Bogdanoff, P. *J. Electrochem. Soc.* **2011**, *158*, B69.
(22) Kramm, U. I.; Herrmann-Geppert, I.; Bogdanoff, P.; Fiechter, S. *J. Phys. Chem. C* **2011**, *115*, 23417.
(23) Jaouen, F.; Herranz, J.; Lefèvre, M.; Dodelet, J.-P.; Kramm, U. I.; Herrmann, I.; Bogdanoff, P.; Maruyama, J.; Nagaoka, T.; Garsuch, A.; Dahn, J. R.; Olson, T. S.; Pylypenko, S.; Atanassov, P.; Ustinov, E. A. *ACS Appl. Mater. Interfaces* **2009**, *1*, 1623.
(24) Wood, T. E.; Tan, Z.; Schmoeckel, A. K.; O' Neill, D.; Atanasoski, R. *J. Power Sources* **2008**, *178*, 510.
(25) Jaouen, F.; Marcotte, S.; Dodelet, J.-P.; Lindbergh, G. *J. Phys. Chem. B* **2003**, *107*, 1376.
(26) Karweik, D. H.; Winograd, N. *Inorg. Chem.* **1976**, *15*, 2336.
(27) Griffiths, D. M.; Standing, H. A. In *Coal Science*; Given, P. H., Ed.; American Chemical Society: Washington D.C., 1966; p 666.
(28) Jaouen, F.; Charreteur, F.; Dodelet, J.-P. *J. Electrochem. Soc.* **2006**, *153*, A689.
(29) Kramm, U. I.; Herrmann-Geppert, I.; Fiechter, S.; Zehl, G.; Zizak, I.; Dorbandt, I.; Schmeißer D.; Bogdanoff, P. *J. Mater. Chem. A*; DOI: 10.1039/C3TA13821F.
(30) Grabke, H. J.; Moszynski, D.; Müller-Lorenz, E. M.; Schneider, A. *Surf. Interface Anal.* **2002**, *34*, 369.
(31) Herrmann, I.; Kramm, U. I.; Radnik, J.; Bogdanoff, P.; Fiechter, S. *J. Electrochem. Soc.* **2009**, *156*, B1283.
(32) Rümmeli, M. H.; Kramberger, C.; Schäffel, F.; Borowiak-Palen, E.; Gemming, T.; Rellinghaus, B.; Jost, O.; Löffler, M.; Ayala, P.; Pichler, T.; Kalenczuk, R. J. *Phys. Status Solidi B* **2007**, *244*, 3911.
(33) Faubert, G.; Côté, R.; Guay, D.; Dodelet, J.-P.; Dénès, G.; Poleunis, C.; Bertrand, P. *Electrochim. Acta* **1998**, *43*, 1969.
(34) Gojkovic, S. L.; Gupta, S.; Savinell, R. F. *J. Electroanal. Chem.* **1999**, *462*, 63.
(35) Borsa, D. M.; Boerma, D. O. *Hyperfine Interact.* **2003**, *151/152*, 31.
(36) Blomquist, J.; Lang, H.; Larsson, R.; Widelöv, A. *J. Chem. Soc., Faraday Trans.* **1992**, *88*, 2007.
(37) Bouwkamp-Wijnoltz, A. L.; Visscher, W.; Veen, J. A. R. v.; Boellaard, E.; Kraan, A. M. v. d.; Tang, S. C. *J. Phys. Chem. B* **2002**, *106*, 12993.
(38) Schulenburg, H.; Stankov, S.; Schünemann, V.; Radnik, J.; Dorbandt, I.; Fiechter, S.; Bogdanoff, P.; Tributsch, H. *J. Phys. Chem. B* **2003**, *107*, 9034.
(39) Ferrandon, M.; Kropf, A. J.; Myers, D. J.; Artyushkova, K.; Kramm, U.; Bogdanoff, P.; Wu, G.; Johnston, C. M.; Zelenay, P. *J. Phys. Chem. C* **2012**, *116*, 16001.
(40) Greenwood, N. N.; Gibb, T. C. *Mössbauer Spectroscopy*; 1st ed.; Chapman and Hall Ltd.: London, 1971; Vol. *1*.
(41) Melendres, C. A. *J. Phys. Chem.* **1980**, *84*, 1936.
(42) Taube, R. *Pure Appl. Chem.* **1974**, *38*, 427.
(43) Lang, G.; Marshall, W. *Proc. Phys. Soc.* **1966**, *87*, 3.
(44) Debrunner, P. G. In *Iron Porphyrins Part 3*; Lever, A. B. P., Gray, H. B., Eds.; Wiley-VCH: Hoboken, NJ, 1989; p 139.
(45) Anderson, A. B.; Sidik, R. A. *J. Phys. Chem. B* **2004**, *108*, 5031.
(46) Meng, H.; Larouche, N.; Lefèvre, M.; Jaouen, F.; Stansfield, B.; Dodelet, J.-P. *Electrochim. Acta* **2010**, *55*, 6450.